Supplemental Information

Materials and Methods:

Design of constructs and molecular dynamics simulation

Before construction of HPAz, an *in silico* model of the protein was generated using VMD package (42). The model was then energy minimized (5000 steps, 2 fsec/step) and simulated for a total of 1 ns, at 310 K with NPT condition using the NAMD software package (43). The mutations were introduced into the Az gene containing a leader sequence to allow periplasmic expression in the pET-9a vector through QuickChange PCR (PfuUltraII, Agilent technologies) and confirmed by DNA sequencing at the CORE DNA sequencing facility (Urbana, IL).

Protein expression and purification

Expression and purification of HPAz was achieved through minor modifications of a previously reported method (44). The HPAz plasmid was expressed in *E. coli* using BL21 (DE3)* chemical competent cells (NEB) transformed with the gene of interest using the standard heat shock method, plated on LB agar plates containing 50 µg/mL of kanamycin and incubated at 37°C overnight to produce single colonies. A single colony was then picked and inoculated in 50 mL LB culture media with 50 µg/mL kanamycin at 37°C overnight. The above 50 mL starter culture was then transferred to a 2 L culture of 2xYT media [16 g/L bactotryptone (BD), 10 g/L yeast extract (BD) and 5 g/L NaCl (Fisher)] containing 50 mg/L kanamycin. The 2 L cultures were incubated with shaking at 25°C until an OD_{600}~1.0-1.5 was reached. The cultures were then induced with 300 mg/L of IPTG (Gold Bio Technology Inc.) and incubation at 25°C was continued overnight.

After expression, the cells were harvested by centrifugation and re-suspended in 1/8 the original culture volume of a recovery solution consisting of 200 g/L sucrose (Fisher), 50 mM Tris buffer at pH 8.0 and 1 mM EDTA (Sigma). The cells were recovered by shaking for 45 minutes at room temperature, and then re-harvested. The periplasmic membrane was ruptured by re-suspending the cells in a solution of 4 mM NaCl and 1 mM DTT (Sigma) and shaking the cells vigorously at 4°C for 20 minutes. After centrifugation, the supernatant containing the Az variant was collected in a separate flask and further purified by adding 1/10 the volume of the supernatant of a 500 mM sodium acetate solution at pH 4.0 to precipitate other components of the cells, which were then removed by centrifugation.

The above supernatant containing the Az variant was then applied to SP-sepharose resin (GE Healthcare) by adding the resin directly to the supernatant and shaking the suspension at 4 °C for at least 2 hours to allow the protein to bind to the resin. The mixture was then packed into a column and the Az variant was purified through a pH gradient from pH 4.1 to pH 6.4 using 50 mM ammonium acetate buffer at the appropriate pH for both washing and eluting. The Az variant was further purified by passing through a Q-sepharose (GE Healthcare) column and a Sephadex S-100 gel filtration column (GE healthcare), both equilibrated in 50 mM ammonium acetate buffer at pH 6.0. The identity of the protein after purification was verified by electrospray ionization mass spectrometry (ESI-MS) (calculated: 13974; observed: 13978 Da). Typical protein yields ranged from 100-200 mg of pure protein per liter of culture and purity was >98 % based on SDS-PAGE.

Due to high affinity of the proteins for Cu, we used a slightly modified protocol for purification of samples for Ni addition. We treated the supernatant before SP column with 1mM EDTA to remove divalent cations. 1 mM EDTA was added to buffers as well. We then purified the protein on a size exclusion column that was previously washed with EDTA and then equilibrated with chelexed buffer. Chelexed buffer was used for eluting the protein from the column as well.

Met121Glu mutant was purified using a different procedure, described previously (45). This modification was necessary to ensure that the protein is purified in its apo form, since this protein has extremely high affinity for divalent metal ions and the procedure used for other variants is not effective to obtain it in the metal-free form.

Copper reconstitution

The Az variant was expressed and purified as apo (metal-free) protein. To reconstitute the copper into the apo-protein, sub-saturating equivalents of either $CuSO_4$ or 5-10 mM $Cu(CH_3CN)_4PF_6$ in acetonitrile was added to the protein solution with stirring in order to minimize the chance that free copper in solution would precipitate the protein.

Ni reconstitution

Ni^{2+} addition to the proteins was performed following a previously reported protocol (34, 35). Briefly, a 50 μM solution of protein in 100 mM phosphate buffer pH 8.0 was prepared. 10 eq. $NiCl_2$ was added to the solution and was stirred for two days at room temperature or 4 °C. As Met121Glu mutant was highly effective at binding to Ni^{2+}, we found that one hour was enough to obtain saturation of the ligand to metal charge transfer band from Ni^{2+} binding.

Mass spectrometry

Electrospray ionization mass spectroscopy (ESI-MS) were obtained on a Quattro II (Waters) ESI mass spectrometer maintained by the School of Chemical Sciences Mass Spectrometry Laboratory (Urbana, IL). For checking the mass of copper free proteins, formic acid was used to ionize the protein upon injection. For observing metal bound proteins, the formic acid was omitted and a solution of the copper bound protein in 5 mM ammonium acetate buffer pH 5.0 was injected as a continuous stream (5 μl/min) via syringe pump to build up sufficient signal to obtain an accurate mass (Figure S14).

Cyclic voltammetry (CV)

For CV on pyrolytic graphite electrodes (CH Instruments, Austin, TX), the electrode was first polished to a mirror finish and until no protein signal was visible. A 1 mM sample of either Cu(II)-HPAz or Cu(I)-HPAz (10 μL) in pH 6.35 ammonium acetate buffer (50 mM) was then added to the exposed carbon and immediately immersed in a solution of 50 mM ammonium acetate buffer at pH 5.0 and 500 mM NaCl. A scan from 0.6 V to 1.3 V vs. the standard hydrogen electrode, SHE, was then run at a scan rate of 0.1 V/sec. No signal was observed in different buffer solutions with carbon electrodes or below a scan rate of 0.1 V/sec. Using faster scan rate of 1V/sec increased the intensity of reductive peak significantly. The CV of Green-Cu(II)HPAz was obtained in 10 mM sodium phosphate buffer at pH 7.0 supplemented with 100 mM sodium formate.

To obtain the potential of Ni-loaded variants, CV was run in 100 mM phosphate buffer at pH 8.0 with 100 mM NaCl, with scan rate of 0.1 V/s. In addition to CV, differential pulse voltammetry (DPV) was performed for Ni-loaded variants to check the accuracy of the peak positions. The DPV parameters are as follows: scan from 0.2 V to -1.2 V with increments of 0.004 V and amplitude of 0.05 V. Pulse width of o.o15 sec was applied with sampling width of 0.005 sec and sampling period of 0.02 sec. A sensitivity of 5e-006 was used.

Software SOAS and OriginPro9.0 were used for data process. Subtraction in SOAS was performed according to the manual. Subtractions in OriginPro were performed using the peak analysis tab. The presence of the peaks was confirmed by taking the first derivative of the voltammagram.

Stopped-flow UV-vis absorption spectroscopy

Stopped-flow UV-vis spectra were collected on an Applied Photophysics Ltd (Leatherhead, UK) SX18.MV stopped-flow spectrometer equipped with a 256-element photodiode array detector. HPAz was concentrated to 0.75 mM in an appropriate buffer and 0.5 mM $Cu(CH_3CN)_4PF_6$ was added by slow addition from a 50 mM stock of the salt in acetonitrile (the solution was sonicated to fully dissolve the Cu(I) salt before the experiment). Sub-saturating equivalents of Cu(I) were used to minimize the chance of free copper in solution to complicate interpretation of the results. Oxidant solutions were prepared in in the appropriate buffer at the appropriate concentrations to deliver the desired number of molar equivalents relative to the amount of Cu(I) in the protein solution upon mixing in the stopped flow chamber. Spectra were collected for up to 1000 seconds with 200 intervals spaced logarithmically with shorter intervals at the start of data collection. A series of chemical oxidants of varying redox potential were used to initially scan for oxidation of reduced HPAz, including $(NH_4)_2Ce(NO_3)_6$ (1.72 V) (46), Ce(IV)/EDTA (1.06 V) (47), Na_2IrCl_6 (0.892 V) (48), $K_2Mo(CN)_8$ (0.798 V) (49), and $K_3Fe(CN)_6$ (0.424 V vs. NHE) (49). In general, oxidants with redox potentials around 0.9 V or higher were able to oxidize Cu(I)-HPAz to varying degrees while lower redox potential oxidants could not. $(NH_4)_2Ce(NO_3)_6$ and Ce(IV)/EDTA only recovered about 10 % of the expected absorbance assuming 100 % oxidation of the protein. Significant scatter was also seen with these titrants, which suggests protein precipitation. Na_2IrCl_6 was seen to yield approximately 20 % of the expected visible absorbance intensity based upon the amount of Cu(I) in solution with one molar equivalent of oxidant. As such, it was used for further spectrochemical titrations. For pH dependent studies of copper oxidation with Na_2IrCl_6 only acetate and phosphate-based buffers were used because Na_2IrCl_6 was seen to react with several other buffering molecules. Cu(II) incorporation was also monitored by stopped-flow by injecting a solution of apo-protein in buffer against a solution of $CuSO_4$.

Because of the instability of the blue Cu(II)-HPAz, we can obtain its E°′ quantitatively using CV, as we can capture the state using a fast scan rate (100 mV/sec), resulting in a largely reversible CV. While redox titrations using oxidants such as Na_2IrCl_6 can in principle obtain the E°′, because the bimolecular redox reaction in solution is much slower, the blue Cu(II)-HPAz, once generated, converted to green Cu(II)-HPAz within the time scale of the redox reaction. Therefore we can estimate the E°′ only semi-quantitatively. Nonetheless, these redox titrations confirm the E°′ obtained from CV is in the correct range.

Spectroscopic studies

Electronic absorption spectra in the UV-visible region (UV-vis) were collected on either an Agilent 8453 diode array (Agilent), a Cary 3E (Varian) or a Cary 5000 (Varian) UV-vis spectrometer. For

the pH dependent studies, a buffer that is effective to maintain pH in a wide range (pH 4-11) without substantially altering the components in solution from sample to sample was used. This buffer (called UB buffer) contained 50 mM sodium acetate, 40 mM MES, 40 mM MOPS, 40 mM Tris, 40 mM CAPS and 100 mM NaCl.

Electron Paramagnetic Resonance (EPR) spectra were collected using an X-band Varian E-122 spectrometer at the Illinois EPR Research Center (IERC). Samples were prepared typically at a final concentration of copper loaded protein of about 0.5-1 mM in the appropriate buffer and frozen as a glass with 20 % glycerol. Spectra were obtained in a temperature independent buffer at pH 7.0 (TIP7) (50) as the effective pH of buffered solutions is known to change substantially when cooled to cryogenic temperatures, which can dramatically alter the observed spectra.

Freeze-quench EPR was performed on a syringe-RAM controller freeze/chemical quench apparatus from Update Instrument, Inc., Madison, WI. Protein sample was prepared in 50 mM phosphate buffer, pH 6.5 with addition of 0.1 M NaCl to decrease the temperature-induced pH changes after freezing. Glycerol was mixed with the protein sample to a final concentration of 10% v/v. Concentrated protein sample loaded with Cu(I) was transferred to a 2 ml syringe and Na_2IrCl_6 to a 0.5 ml syringe at 4X the concentration of the protein. The samples were mixed with a ram speed of 1.6 cm/s using a reactor tube size of 6.4 with a calculated volume of 5.3 μL. The displacement was set such that the reaction time is less than 20 msec and quenched by spraying into a pre-chilled EPR tube filled with iso-pentane cooled in an iso-pentane bath at -120°C. Calculating the time from the initial mixing in the reaction chamber and adding the time required to freeze, a sample time of 20 msec was attained. The frozen sample was packed into a compressed layer in an EPR tube.

Cu K-edge (8.9 keV) extended x-ray absorption fine structure (EXAFS) and x-ray absorption near edge (XANES) data were collected at the Stanford Synchrotron Radiation Lightsource operating at 3 GeV, with currents near 500 mA maintained by continuous top off. Samples were measured as aqueous glasses in 20% ethylene glycol at 10K. All edges were measured on beamline 7-3, using a Si[220] monochromator. All data were collected in fluorescence mode using a high-count rate Canberra 30-element Ge array detector with maximal count rates per array element of <120 kHz. For each edge, four to six scans of buffer blank were averaged and subtracted for all protein samples in order to remove the Z-1 filter Kβ fluorescence and produce a flat pre-edge baseline. A Cu foil was placed between the first and second ionization chamber in order to provide energy calibration. Cu K-edges were collected using an Rh-coated mirror upstream with a 12.5 KeV energy cutoff to reject harmonics, and a nickel oxide filter and Soller slit inserted in front of the detector in order to reduce elastic scattering relative to the Cu Kα fluorescence.

Data averaging, background subtraction, and normalization to the smoothly varying background atomic absorption were performed using EXAFSPAK(51). For the experimental energy threshold energy (k=0), 8995 eV was selected. Spectral simulation was carried by least-squares curve fitting, utilizing full curved wave calculations as formulated by the SRS library program EXCURVE 9.2 (52) as previously described(31). We refined the parameters of the fit as follows: E_0, the photoelectron energy threshold, R_i the distance from the central metal atom (Cu, Se, or Ag) to atom *i* and $2\sigma_2^i$ the Debye-Waller (DW) term for atom *i*. Coordination numbers were fixed to those previously established from crystal structures whenever possible. The quality of the fits was determined using the least-squares fitting parameter, F, which is defined as:

$$F^2 = (1/N)\ \sum_i k^6(\chi_i^{theory} - \chi_i^{experiment})^2$$

and is hereafter referred to as the fit index or fit (FI).

Supplemental figures:

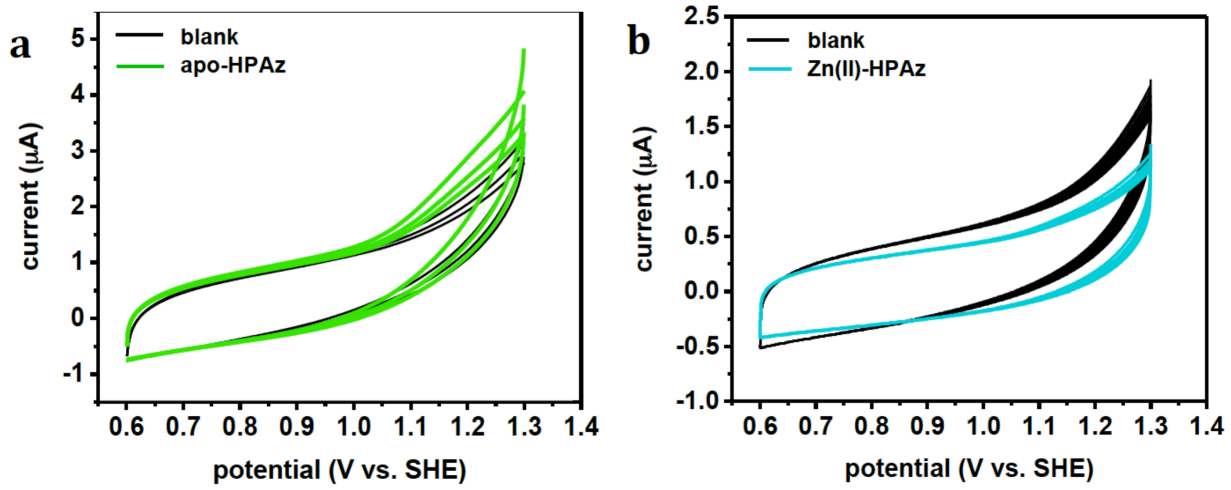

Figure S1. Cyclic voltammagram of Cu-HPAz and associated controls. (a) electrode without protein (Blank) or in the presence of apo-HPAz , (b) Blank or Zn(II)-HPAz, at pH 5.0 in 50 mM ammonium acetate buffer, obtained at scan rate of 0.1 V/sec.

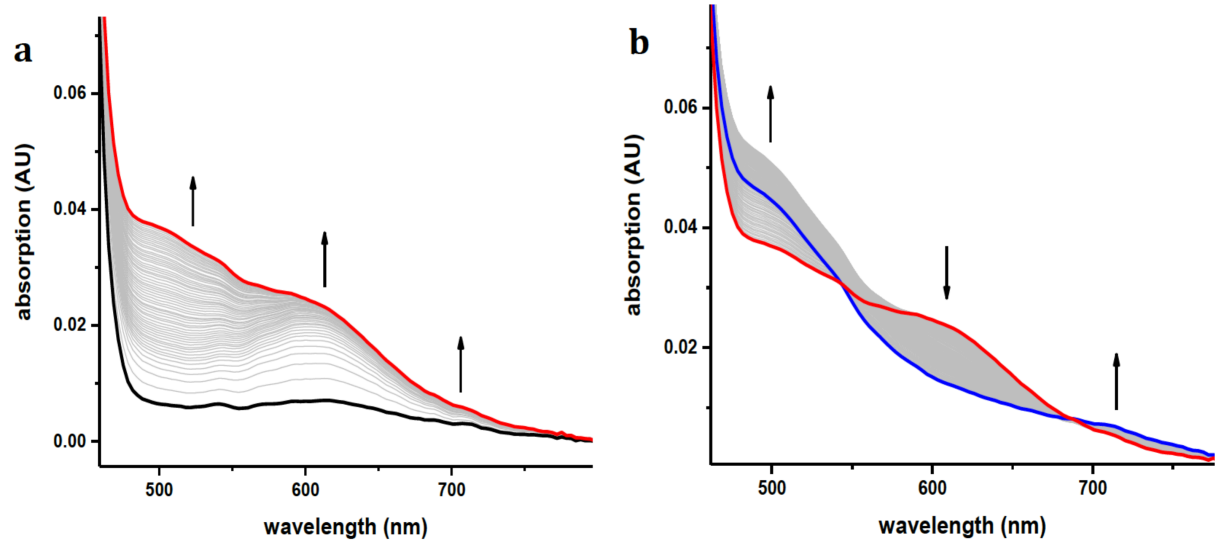

Figure S2. Stopped-flow UV-vis kinetics of Cu(I)-HPAz oxidation by ferricyanide. Reaction of reduced HPAz with 10 molar equivalents of ferricyanide for a) the 1st 20 s (black trace to red trace) and b) from 20 seconds to 1000 seconds (red trace to blue trace).

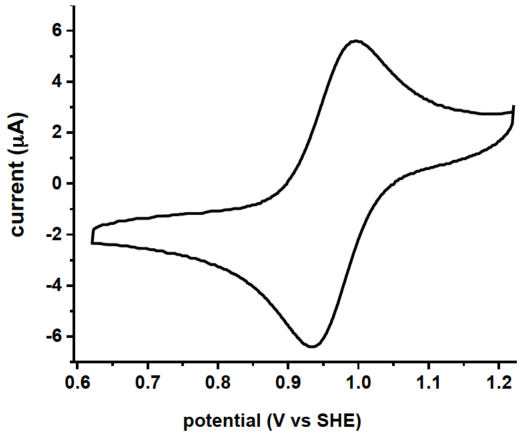

Figure S3. Sample voltammagram of Na_2IrCl_6. Spectrum taken in 50 mM NH_4OAc buffer pH=5.0 + 500 mM NaCl. E_m = 0.96 ± 0.0.

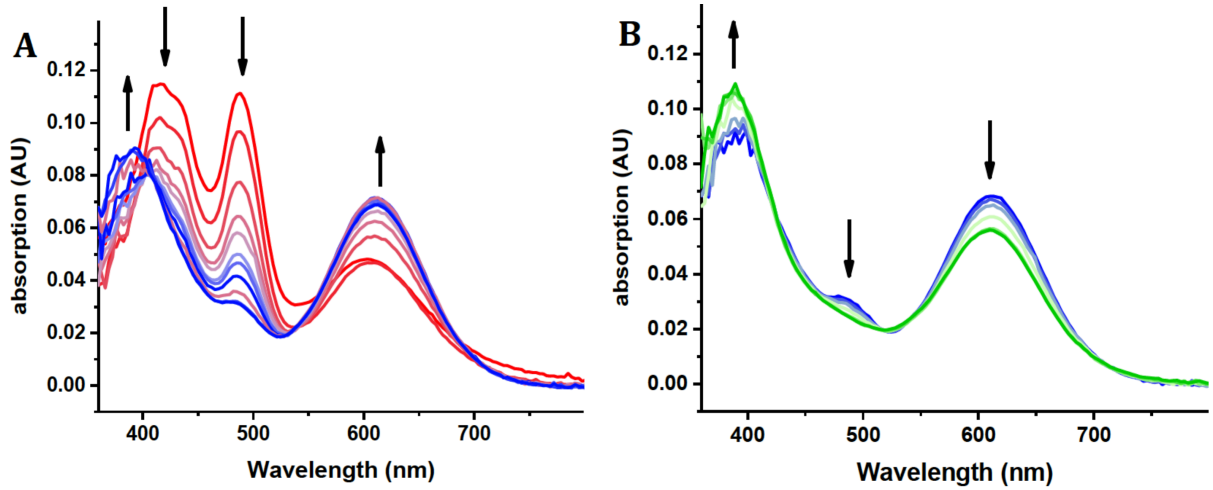

Figure S4. Stopped-flow UV-vis kinetics of oxidation of Cu(I)-HPAz by Na_2IrCl_6. (A) First 10 msec and (B) 10 msec to 10 s oxidation of Cu(I)-HPAz by Na_2IrCl_6 at pH 5.0 ammonium acetate buffer.

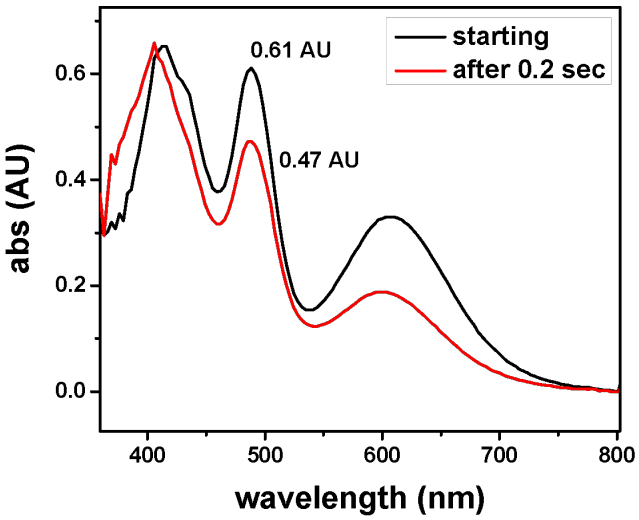

Figure S5. 1:1 reaction of Cu(I)-HPAz and Na_2IrCl_6 resulted in ~25% loss of Na_2IrCl_6 signal after 0.2 sec. The reaction was monitored using stopped-flow. 0.2 sec was used as an end-point to measure the %loss of Na_2IrCl_6 for different reactions with a range of molar equivalents of Na_2IrCl_6.

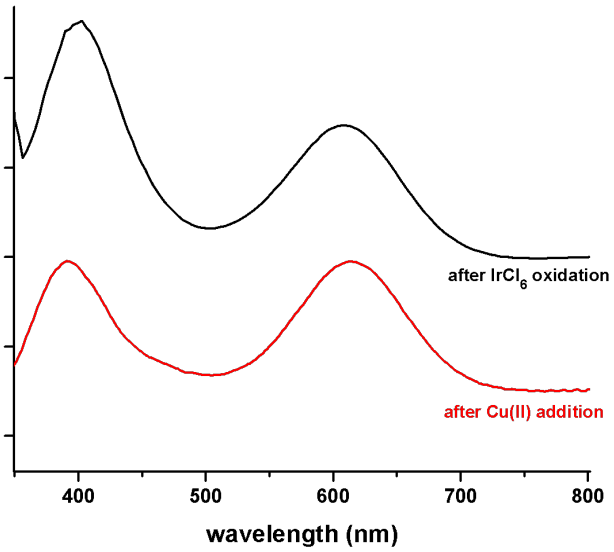

Figure S6. Comparison of the final visible spectra of reoxidized Cu(II)-HPAz and reconstituted Cu(II)-HPAz after addition of Cu(II) to apo-HPAz. The UV-vis spectrum of the reoxidized sample was obtained by reacting the Cu(I)-HPAz sample with Na_2IrCl_6, measured by a stopped-flow visible absorption spectrometer. Because this stopped-flow visible absorption spectrometer is not equipped with a UV lamp, it has a high signal background in region around 400 nm and below, causing the higher relative intensity of the peak ~ 400 nm than the spectrum of reconstituted Cu(II)-HPAz, which was collected on a Cary5000 spectrometer that has a UV lamp and this lower signal background around 400 nm. Moreover, some unreacted Na_2IrCl_6, which has absorbance ~ 400 nm, might be present in the time scale shown, further contributing the increase of absorption in that region in the spectrum.

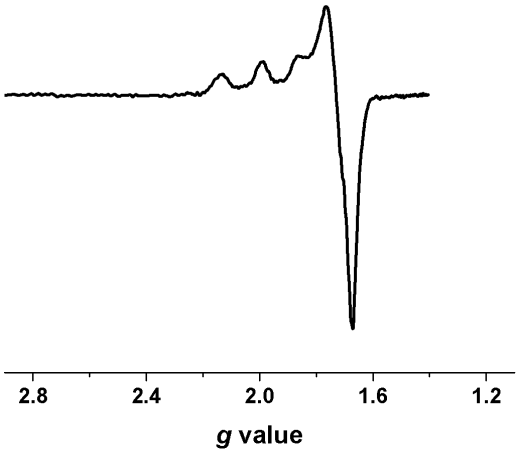

Figure S7. EPR spectrum of Cu(II)-HPAz. Sample is at 50 mM phosphate pH6.5 with 100 mM NaCl, recorded at 30 °K.

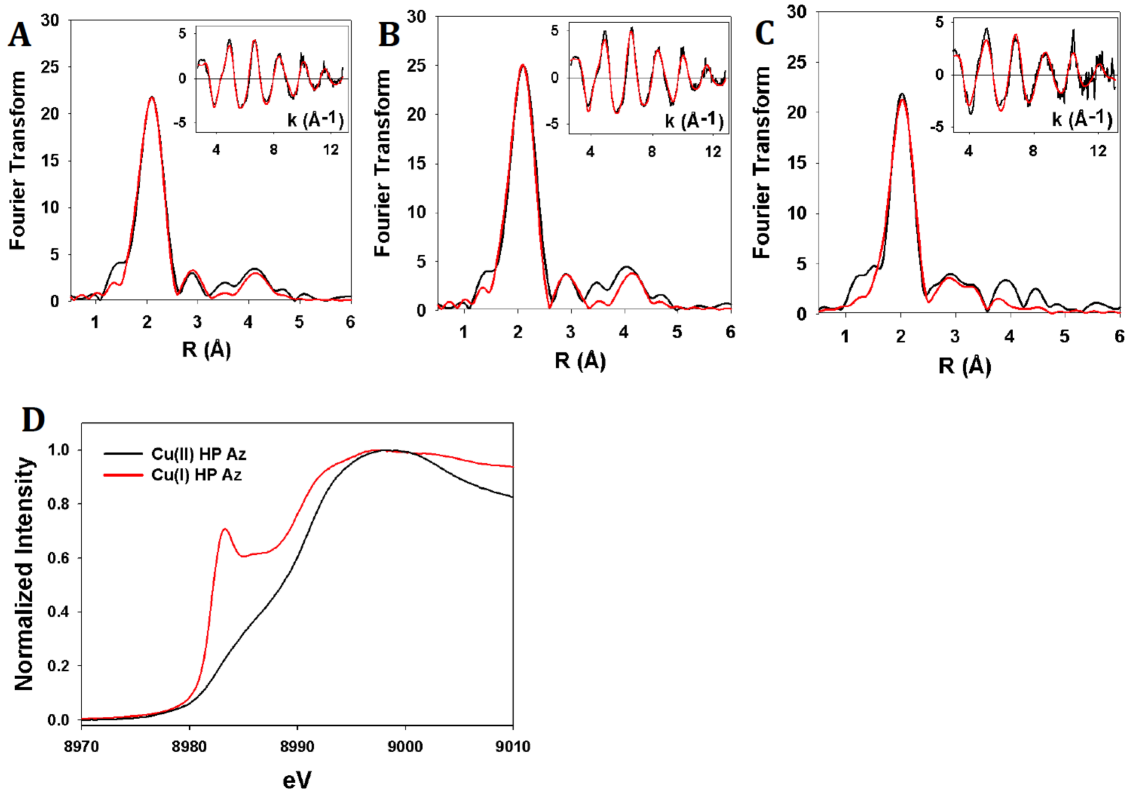

Figure S8. EXAFS and XANES analyses of different HpAz variants. Fourier transform and EXAFS (inset) for (a) Cu(I)-HPAz at phosphate buffer pH 6.5, (b) Cu(I)-HPAz at phosphate buffer pH 8, and (c) Cu(II)-HPAz at phosphate buffer pH 6.5. Experimental data are shown as solid black lines and simulation are shown as solid red lines. Parameters used to fit data were shown in Table 1. (c) Normalized edge spectra for (a) (red line) and (c) (black line).

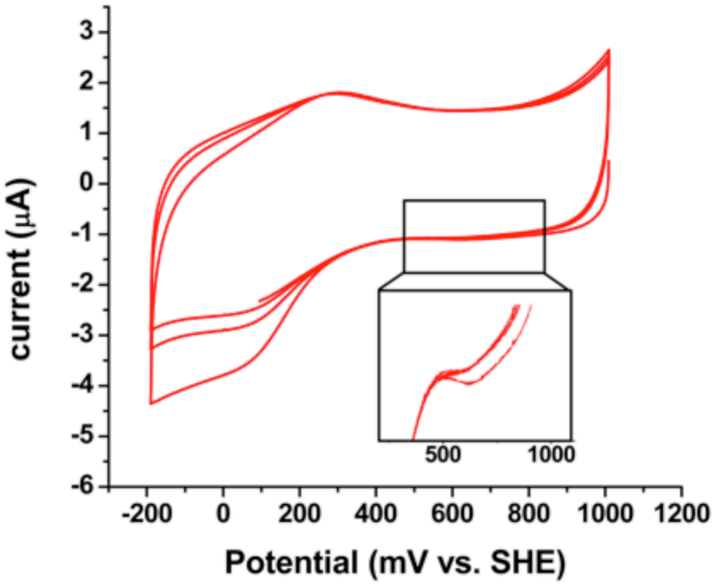

Figure S9. Cyclic voltammagram of Green Cu(II)-HPAz shows a weak reductive peak at 700 mV. CV was performed in 10 mM sodium phosphate buffer pH 7 supplemented with 100 mM sodium formate. The reductive peak is small but it is reproducible. The peaks close to 200 mV are present in the blank electrode as well and are a result of some oxidized functionalities on the electrode surface.

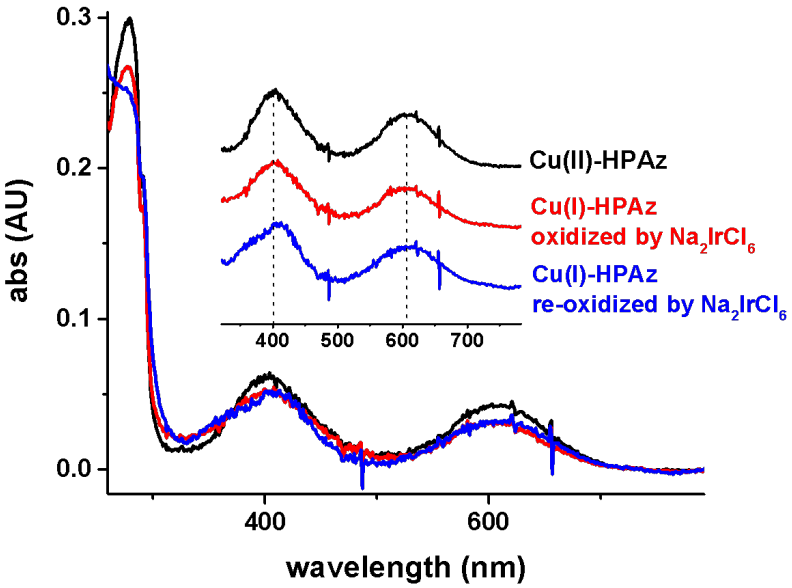

Figure S10. Oxidation and reduction studies of the Green Cu(II)-HPAz. The apo-protein loaded with Cu(I) and then oxidized by Na_2IrCl_6 (the red line) shows similar features to Cu(II)-HPAz at resting state (the black line). The protein can go back to the resting state after being reduced by ascorbate and then being oxidized back by Na_2IrCl_6 (the blue line).

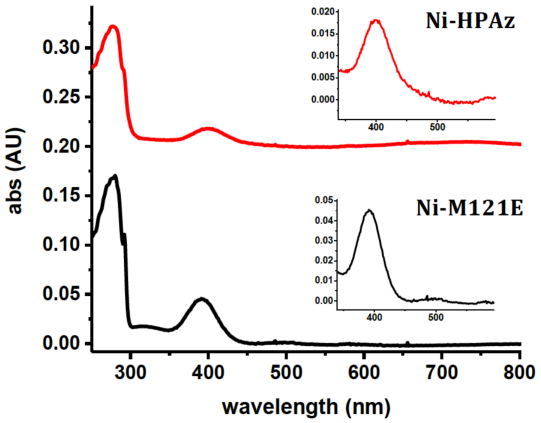

Figure S11. Representative UV-vis spectra of Ni-HPAz and Ni-M121E.

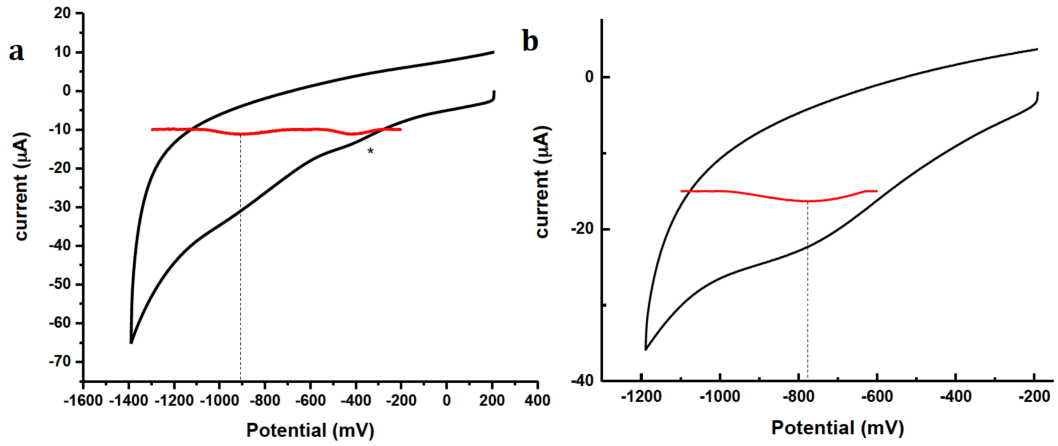

Figure S12. Representative cyclic voltammagram of Ni-Az variants, (a) Ni-Met121Glu and (b) Ni-WTAz, obtained at 100 mM phosphate buffer at pH 8.0 with 100 mM NaCl, at scan rate of 0.1 V/s. The red trace is after subtracting the capacitative current. As shown in the figures, only a reductive peak is observable, because the oxidative peak was not observed due to high reactivity and instability of Ni(I) state of the samples. The peak shown with * in Met121Glu spectra is observed in the blank as well. The values for Ni-loaded Az variants are based on the reductive peak position, as the Ni^{+} state is not stable.

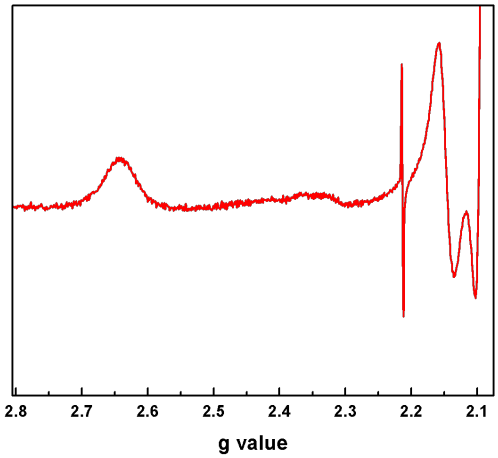

Figure S13. EPR of Ni-M121E after cryo-reduction shows features of Ni(I). (power 20db, modulation 4, 15 °K). The sharp feature at around g=2 and the smaller one at g=2.2 are due to radiolytically generated free radicals and hydrogen in quartz EPR tube, respectively.

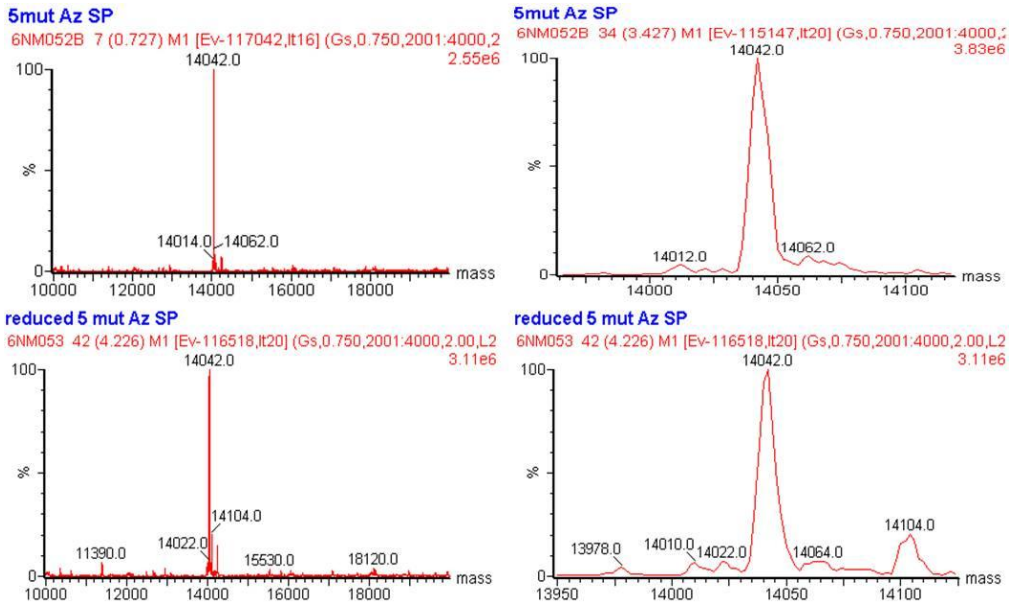

Figure S14. Mass spectroscopy study of Cu-HPAz. Syringe-pump ESI-MS of Cu(II)-HPAz (top) and Cu(I)-HPAz (bottom showing that one Cu is bound to the protein (MW= 14036 [13973 apo-HPAz+ 68 Cu])

Supplemental tables:

Table S1. EPR simulation parameters of 20 msec freeze quenched sample.

Species	**%**	**g_x, g_y, g_z**	**A_x, A_y, A_z (10^{-4} cm^{-1})**
Final species (T2 Cu like)	39	2.009, 2.079, 2.230	0.14, 11.46, 144.81
T1 Cu like	60	2.021, 2.069, 2.309	23.04, 25.23, 65.19
Free-radical like	1	2.011, 2.003, 1.992	0.00, 0.00, 0.00

Table S2. Simulation paramters of EPR spectrum of the final product of Cu-HPAz oxidation at 50 mM phosphate pH6.5 with 100 mM NaCl, recorded at 30 °K.

Species	**%**	**g_x, g_y, g_z**	**A_x, A_y, A_z (10^{-4} cm^{-1})**
Final species (T2 like)	74	2.009, 2.079, 2.230	0.14, 11.46, 144.81
T1 like	26	2.021, 2.069, 2.309	23.04, 25.23, 65.19

References:

1. Humphrey W, Dalke A, & Schulten K (1996) VMD: visual molecular dynamics. *J. Mol. Graphics* 14(1):33-38, 27-38.
2. Phillips JC*, et al.* (2005) Scalable molecular dynamics with NAMD. *J. Comput. Chem.* 26(16):1781-1802.
3. Hay M, Richards JH, & Lu Y (1996) Construction and characterization of an azurin analog for the purple copper site in cytochrome c oxidase. *Proc. Natl. Acad. Sci. U. S. A.* 93(1):461.
4. Lancaster KM, George SD, Yokoyama K, Richards JH, & Gray HB (2009) Type-zero copper proteins. *Nature Chem.* 1:711-715.
5. Czernuszewicz RS, Fraczkiewicz G, & Zareba AA (2005) A detailed resonance Raman spectrum of Nickel(II)-substituted Pseudomonas aeruginosa azurin. *Inorg. Chem.* 44(16):5745-5752.
6. Moratal JM, Romero A, Salgado J, Perales-Alarcon A, & Jimenez HR (1995) The crystal structure of nickel(II)-azurin. *Eur. J. Biochem.* 228(3):653-657.
7. Lide DR & Frederikse HPR (1997) *Handbook of Chemistry and Physics* (CRC Press).
8. Abbaspour A & Mehrgardi MA (2005) Electrocatalytic activity of Ce(III)-EDTA complex toward the oxidation of nitrite ion. *Talanta* 67(3):579-584.

9. Bossu FP, Chellappa KL, & Margerum DW (1977) *J. Am. Chem. Soc.* 99:2195.

10. Robert S, Peter YEH, & Theodore K (1977) Evaluation of Mediator-Titrants for the Indirect Coulometric Titration of Biocomponents. *Electrochemical Studies of Biological Systems,* ACS Symposium Series, (AMERICAN CHEMICAL SOCIETY), Vol 38, pp 143-169.

11. Sieracki NA, Hwang HJ, Lee MK, Garner DK, & Lu Y (2008) A temperature independent pH (TIP) buffer for biomedical biophysical applications at low temperatures. *Chem Commun (Camb)* (7):823-825.

12. George GN (1990) EXAFSPAK (Stanford Synchrotron Radiation Laboratory, Menlo Park, CA).

13. Binsted N, Gurman SJ, & Campbell JW (1998) EXCURVEWarrington, UK).

14. Clark KM*, et al.* (2010) Transforming a blue copper into a red copper protein: engineering cysteine and homocysteine into the axial position of azurin using site-directed mutagenesis and expressed protein ligation. *J. Am. Chem. Soc.* 132:10093-10101.